The effects of liquid water on the NDSA method for measuring tropospheric water vapor along LEO-LEO satellite links

Fabrizio CUCCOLI [(a)], Luca FACHERIS [(b)]
[(a)] CNIT O.U. c/o Department of Electronics and Telecommunications, Via di Santa Marta, 3, 50139 Firenze, Italy, email: fabrizio.cuccoli@ unifi.it
[(b)] Department of Electronics and Telecommunications, Via di Santa Marta, 3, 50139 Firenze, Italy, email: facheris@ingfi1.ing.unifi.it

ABSTRACT

The NDSA (Normalized Differential Spectral Absorption) method has been proposed for estimating the total content of water vapor (*IWV*, Integrated Water Vapor) along a tropospheric propagation path between two Low Earth Orbit (LEO) satellites. This method requires a transmitter onboard the first LEO satellite and a receiver onboard the second one. It is based on the simultaneous measurement of the total attenuation at two relatively close frequencies in the Ku/K bands, and on the estimate of a parameter referred to as 'spectral sensitivity'. This approach is potentially able to emphasize the water vapor contribution, to cancel out all spectrally flat unwanted contributions and to limit the impairments due to tropospheric scintillation. The objective of this paper is to analyze the effects of liquid water presence along the propagation LEO-LEO link on the NDSA approach. Results are based on computer simulation and account for different frequency carriers in the 15-30 GHz range and for any value of liquid water content along the propagation path at 3 km tangent altitude.

Keywords: water vapor, trosposphere, meteorological remote sensing, trace gas, satellite sensing

1. INTRODUCTION

Recently, we introduced the Normalized Differential Spectral Absorption (NDSA) concept for retrieving the total content of water vapor (*IWV*, Integrated water vapor) along the propagation path between two Low Earth Orbiting (LEO) satellites[(1)]. NDSA is based on the simultaneous measurement of the total attenuation at two relatively close frequencies in the *Ku/K* bands, and on the estimate of a "spectral sensitivity parameter" that is highly correlated to the *IWV* content of the LEO-LEO link in the low troposphere. The NDSA approach has the potential to overcome all spectrally 'flat' and spectrally correlated phenomena, and its potentiality has been well verified in absence of liquid water along the LEO-LEO link using numerical simulations based on atmospheric propagation models and radiosonde profile data[(2)].
In this paper, after having recalled the basic concepts of the *IWV* estimation by NDSA measurement, we focus our attention on the effects of the presence of liquid water along the propagation path. In particular we quantify the effects on the spectral sensitivity parameter due to the liquid water content for each frequency considered.
Also, we discuss about the possibility to retrieve separately the liquid water content and the water vapor content using at least two NDSA measurement in two separated *Ku/K* band frequency channels between 15 and 30 GHz.
The results will be based on numerical simulations based on the MPM93 propagation model, real atmospheric profiles and a simplified propagation geometry.

2. NDSA RATIONALE AND BASIC EQUATIONS

For a microwave transmitter-receiver link, the radiative transfer equation providing the expected power spectral density $P_{tx}(f)$ at the receiver can be arranged in the following form[(3,4)]

$$P_{rx}(f) = \alpha(f) P_{tx}(f) \exp(-\tau_a(f)) \quad (1)$$

Remote Sensing of Clouds and the Atmosphere X, edited by Klaus Schäfer, Adolfo Comerón, James R. Slusser, Richard H. Picard, Michel R. Carleer, Nicolaos Sifakis,
Proc. of SPIE Vol. 5979, 59790P, (2005) · 0277-786X/05/$15 · doi: 10.1117/12.626997

where f is the frequency, $P_{tx}(f)$ is the transmitted spectral power, $\tau_a(f)$ is the optical depth related to the propagation link and due to atmospheric absorption, while $\alpha(f)$ is the contribution due to all effects different from gaseous absorption (i.e., scattering, antenna gains, defocusing, etc.). In the frequency range considered (15-30 GHz), the optical depth depends on the absorption due to water vapor, to O2 and N2.
After (1), the total spectral attenuation $A(f)$ for the given link is defined as:

$$A(f) = \frac{P_{tx}(f)}{P_{rx}(f)} = \frac{exp(\tau_a(f))}{\alpha(f)} \tag{2}$$

Throughout the paper, the 2D geometry of Fig. 1 is considered, with the two satellite orbits assumed circular. This geometry holds both to a counter-rotating and a co-rotating satellite pair, since the basic NDSA method is independent of the relative motion and can be thus applied in both cases. For simplicity, we assume that the propagation path is rectilinear: such hypothesis, that speeds up significantly the simulations of propagation (which is fundamental to analyze a high number of atmospheric profiles), has no practical impact on the objective of interest (the relationships used to retrieve the *IWV* by means of NDSA measurements and the effects of liquid water on such relationships).

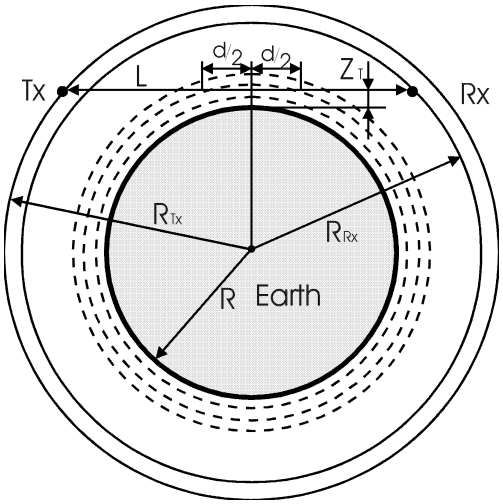

Figure 1: Geometry and parameters of a LEO-LEO link (with simplified rectilinear radio propagation path). Satellites can be co-rotating or counter-rotating

Let us therefore define the spectral sensitivity function $S(f)$ as:

$$S(f) = \frac{1}{A(f)} \frac{d}{df} [A(f)] \tag{3}$$

If $d\alpha(f)/df \cong 0$ in the frequency region of interest, $S(f)$ becomes:

$$S(f) = \frac{d}{df} [\tau_a(f)] \cong \frac{d}{df} [\tau_{aH_2O}(f)] \tag{4}$$

which shows that the spectral sensitivity function is independent of any frequency-flat contribution, while depends directly on the absorption optical depth contributed by water vapor only along the given propagation path. It is therefore reasonably expected that by estimating $S(f)$ (or an approximate version) at one or more frequencies, one can obtain information that is correlated only to the water vapor content along the propagation path under exam. In practice, from (3), the following simple approximate version of $S(f)$ can be used:

$$\hat{S}(f_o) = \frac{A(f_+) - A(f_-)}{2\Delta f\, A(f_+)} \tag{5}$$

where f_o is the reference central frequency (the carrier frequency hereon) while $f_+ = f_o + \Delta f$ and $f_- = f_o - \Delta f$. Obviously, Δf must be small enough so that the spectral derivative in (3) can be well approximated by a finite difference.

Figure 2 shows the differential attenuation and the corresponding spectral sensitivity versus f_o, for tangent altitudes from 0 to 10 km with $2\Delta f$=200 MHz. Evidently, at each tangent altitude z_T we have a value of f_o giving the maximum value of $\hat{S}(f_o)$. Moreover, observing Fig. 2 we can notice that:

- For any given tangent altitude, carrier frequencies lower than 15 GHz bring values of differential attenuation and spectral sensitivity that are more than one order of magnitude smaller than the maximum;

the maxima of the differential attenuation and of the spectral sensitivity curves fall between 21 and 22 GHz, depending on z_T.

In the following section we proceed by analyzing the quantitative impact of natural variations of the atmospheric profiles on $\hat{S}(f_o)$ in no disturbance conditions (infinite SNR at the receiver and no scintillation impairments).

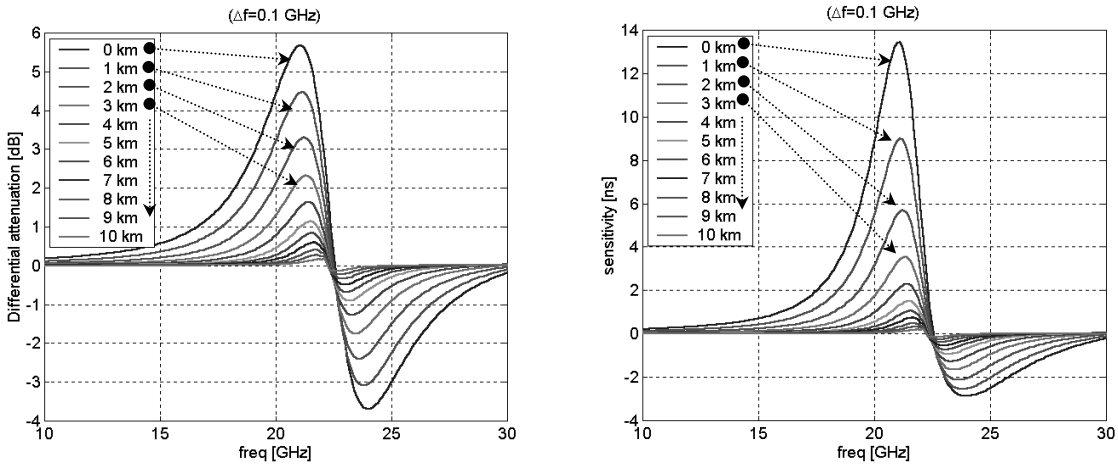

Figure 2: Left plots: differential attenuation (in dB) versus center frequency f_o for $2\Delta f$=200 MHz Right plots: the corresponding spectral sensitivity (as from eq. (5)). Such plots are obtained under the hypotheses of MLS atmospheric model profiles, rectilinear propagation path, spherical symmetry and MPM93 propagation model [5].

3. THE *IWV-S* RELATIONSHIPS

We accounted for the natural variations of the atmospheric conditions by means of real radiosonde data, extended to the whole Earth's atmosphere through the spherical symmetry hypothesis. Vertical profiles of temperature (T), pressure (P) and water vapor concentration (N_w) come from more than 8000 real radiosonde observations made in 20 sites at different latitudes in the northern hemisphere with a resolution of at least 250 m. The latitude of the radiosonde sites ranges from 5 to 80 degrees and all seasonal and day/night atmospheric conditions are accounted for by such measurements. For each site, we used all available measurements of the year 2002 (data taken from the web site of the FSL/NCDC Radiosonde Data Archive[6]). We used the Millimeter wave Propagation Model-version 1993 (MPM93) [5] to compute the total attenuation at both f_+ and f_- along the rectilinear LEO-LEO propagation link, then we computed the spectral sensitivity according to eq. (5). We then simulated the NDSA measurements along the LEO-LEO links at tangent altitudes from 1 to 11 km (step 2 km) and for carrier frequencies from 15 to 25 GHz (step 2 GHz).

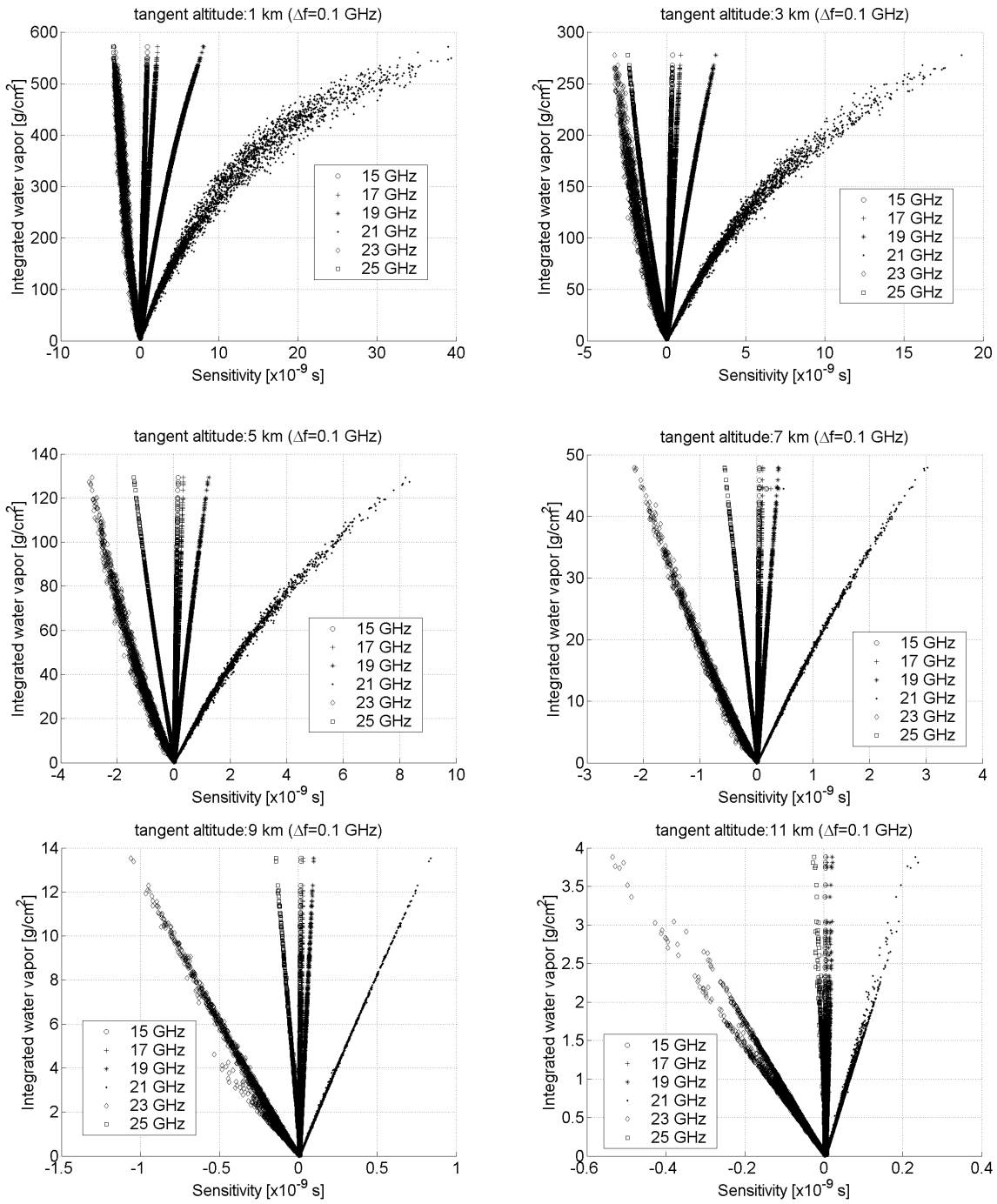

Figure 3: scatter plots of *IWV* versus spectral sensitivity for $2\Delta f$=200 MHz for z_T from 1 to 11 km, step 2 km and for f_o from 15 to 25 GHz, step 2 GHz.

Figure 3 shows all the scatter plots of *IWV* versus spectral sensitivity for all the f_o-z_T combinations and for a spectral separation 2Δf =200 MHz. The basic outcome of the qualitative analysis of such results is that for several f_o-z_T combinations, the correlation between $\hat{S}(f_o)$ and *IWV* is so high that these two parameters can be considered as deterministically related over a wide range of atmospheric profiles, accounting even for their latitude and daily/seasonal variations. Table 1 shows the (linear) correlation coefficients for each of the scatter plots in fig. 3. For all f_o-z_T pairs exhibiting correlation values close to 1, a linear relationship can be used to convert $\hat{S}(f_o)$ to *IWV*: the shadowed cells show the f_o-z_T pairs with a correlation coefficient greater than 0.995.

Tangent altitude [km]	**Frequency**					
	15 GHz	**17 GHz**	**19 GHz**	**21 GHz**	**23 GHz**	**25 GHz**
1	0.9984	0.9983	0.9944	0.9665	0.9730	0.9897
3	0.9986	0.9991	0.9983	0.9798	0.9843	0.9964
5	0.9988	0.9994	0.9994	0.9919	0.9897	0.9990
7	0.9973	0.9991	0.9997	0.9983	0.9944	0.9998
9	0.9522	0.9844	0.9972	0.9997	0.9952	0.9969
11	0.7085	0.8153	0.9438	0.9970	0.9927	0.9518

Table 1: correlation coefficients corresponding to each of the scatter plots in figure 3. The shadowed cells are those with values >0.995.

From a quantitative point of view, we considered for all the f_o-z_T pairs both a linear and a quadratic relationship giving an estimate of *IWV* from $\hat{S}(f_o)$:

$$\hat{IWV} = a_1 \hat{S}(f_0) + a_1 \tag{6}$$

$$\hat{IWV} = b_2 \left[\hat{S}(f_0)\right]^2 + b_1 \hat{S}(f_0) + b_o \tag{7}$$

Then we expressed the error associated with the estimate provided by the *IWV-S* relationships above, with the following percentage relative error:

$$re = \frac{std(\hat{IWV} - IWV)}{mean(IWV)} \cdot 100 \tag{8}$$

Table 2 shows the relative error in the linear relationship case. The two lowest *re* values are evidenced for each of the six frequencies considered: notice that the optimal f_o-z_T combinations of Table 2 correspond to those evidenced in Table 1, which confirms the tight linear relationship between *S* and *IWV* occurring for those combinations.
Table 3 shows the relative error obtained applying the quadratic relationship. As in Table 2, the two lowest *re* values are evidenced for each value of f_o. The shaded cells indicate the f_o-z_T pairs at which the use of a quadratic relationship brings a significant improvement with respect to the linear relationship (*re* reduced by more than 50%). Considering the small error obtained, in these cases it is convenient to use a quadratic relationship instead of a linear one, even if it requires that the additional coefficient b_2 be estimated.
For each tangent altitude it is thus possible to determine the optimal frequency to estimate the *IWV* directly from spectral sensitivity measurements in the ideal case (no receiver nor propagation disturbances). Obviously, at the parity

of *re*, the frequency providing the *IWV-S* relationship with smaller slope should be preferred since this minimizes the effects on the *IWV* estimates due to uncertainties on the spectral sensitivity measurements.

Tangent altitude [km]	**Frequency**					
	15 GHz	**17 GHz**	**19 GHz**	**21 GHz**	**23 GHz**	**25 GHz**
1	**5.7**	5.7	10.4	25.4	22.8	14.6
3	**5.5**	**4.3**	6.1	20.9	18.4	8.9
5	5.9	**4.1**	**4.0**	15.2	17.2	**5.3**
7	9.7	5.6	**3.3**	7.8	14.1	**2.8**
9	40.1	23.1	9.8	**2.9**	**12.8**	10.3
11	74.9	61.5	35.1	**8.3**	**12.8**	32.6

Table 2: relative error *re* [%] for different frequency-tangent altitude combinations. The linear relationship (6) has been used; the coefficients a_1 and a_0 have been computed through linear fit applied to the scatter plots of figure 3. Bold underlined values are the two lowest errors for each column.

Tangent altitude [km]	**Frequency**					
	15 GHz	**17 GHz**	**19 GHz**	**21 GHz**	**23 GHz**	**25 GHz**
1	**3.8**	**2.4**	**1.7**	10.1	19.8	4.5
3	**4.7**	**3.2**	**1.2**	7.7	14.2	4.7
5	5.4	3.5	**1.7**	4.7	**10.5**	**0.9**
7	9.6	5.6	2.9	**2.5**	**8.4**	**2.5**
9	26.3	18.7	9.6	**1.9**	10.8	9.4
11	70.9	56.1	33.1	8.3	12.4	32.3

Table 3: relative error *re* [%] for different frequency-tangent altitude combinations. The quadratic relationship (7) has been used; the coefficients b_2 , b_1 and b_0 have been computed through quadratic fit applied to the scatter plots of figure 3. Bold underlined values are the two lowest errors for each column. Shaded cells indicate the frequency-altitude combinations at which *re* is reduced by more than 50% with respect to the linear fit case (see Table 2).

4. THE EFFECT OF LIQUID WATER ON THE SPECTRAL SENSITIVITY

The presence of liquid water along the LEO-LEO propagation path cannot be in general excluded at the lowest tangent altitudes, due the presence of clouds and/or rainfall. Since the spectral attenuation due to liquid water varies with frequency, clouds and rainfall have an impact on spectral sensitivity measurements, and it is therefore needed to understand to which extent they may influence the *IWV-S* relationships. Since the attenuation due to rainfall is very high in the *Ku/K* bands, while clouds give rise to a relatively low contribution of attenuation at the parity of extension, it is expected that spectral sensitivity measurements are extremely degraded and not utilizable when the propagation path intercepts rainfall cells; on the other hand, this occasional drawback is limited to the lowest tangent altitudes. For this reason, here we focus only on the impact of clouds liquid water content on spectral sensitivity.

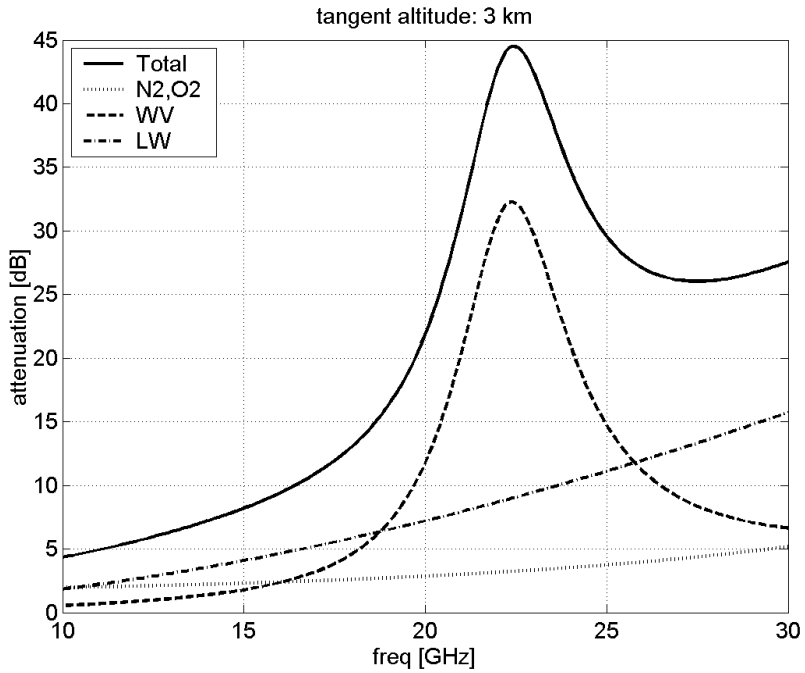

Figure 4: total spectral attenuation in dB with separate contributions due to water vapor, liquid water vapor and N_2/O_2 computed at z_T= 3 km under the following hypotheses: constant (0.1 g·m-3) liquid water content from 3 to 4 km altitude, MLS atmospheric model profiles, rectilinear propagation path, spherical symmetry and MPM93 propagation model.

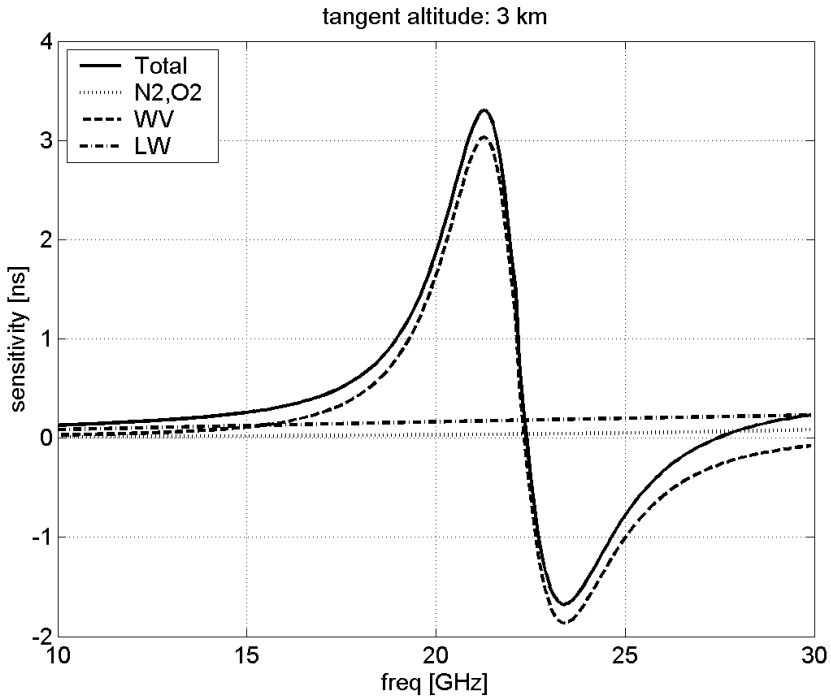

Figure 5: total spectral sensitivity (with $2\Delta f$=200 MHz) with separate contributions due to water vapor, liquid water vapor and N_2/O_2 computed at z_T= 3 km under the same assumptions of figure 4.

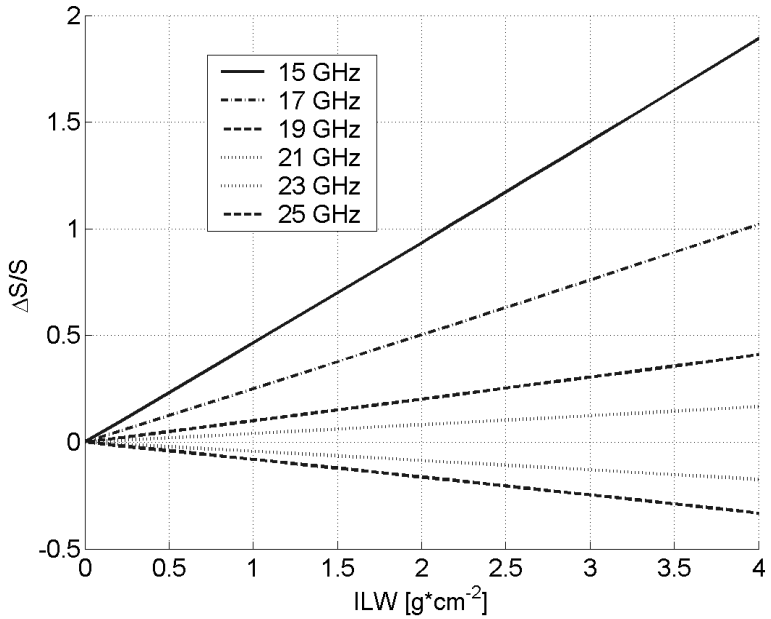

Figure 6: relative variation of the spectral sensitivity versus the liquid water content of the propagation path, for the considered frequencies.

Figures 4 and 5 show respectively the attenuation and the spectral sensitivity (still computed by means of the MPM93) for a LEO-LEO link at z_T=3 km in the presence of 2.25 g·cm^{-2} integrated liquid water (*ILW*); also the other contributions to the total attenuation are shown. The MLS atmospheric model is assumed for the dry air contribution.
Evidently, the contribution of liquid water to the total attenuation varies with frequency, though such variation is much less pronounced than that due to the presence of water vapor. The effect of liquid water on the total spectral sensitivity is a positive bias. In particular, the *ILW* contribution dominates around 30 GHz: therefore, from a theoretical point of view such carrier frequency could be exploited to detect the presence of liquid water along the radio path. Figure 6 shows how *S* varies with the *ILW* for all frequencies considered before. In general it is worth observing that the *ILW* effects on *S* are opposite in correspondence to two carrier frequencies lying on two opposite sides with respect to the 22.235 GHz absorption peak. This could be exploited in a multi-carrier approach to reduce the impact of the *ILW* on the spectral sensitivity measurements used to estimate *IWV*.

5. CONCLUSIONS

The NDSA approach, based on the high correlation between *S* and *IWV*, is attractive for estimating the water vapor content along a given transmitter-receiver link crossing the lowest troposphere.
Simulations have clearly confirmed that *IWV* is related to *S* through a linear or quadratic relationship at any altitude up to 11 km, on a global scale. Since the number of tropospheric layers crossed by the propagation path decrease with the tangent altitude, the carrier frequency giving the least error also depends on the altitude interval of interest, as a direct consequence of the variation with height of the atmospheric parameters.
At the very lowest tangent altitudes the presence of liquid water along the propagation path affects spectral sensitivity measurements since the spectral attenuation due to liquid water varies with frequency. The effect on the spectral sensitivity is a positive bias depending on the liquid water content. Therefore, single NDSA carrier measurements would bias the *IWV* estimate. However, it is envisaged that a multi-carrier NDSA approach could help to detect the presence of liquid water and/or mitigate its effects on the *IWV* estimates.

REFERENCES

1. F. Cuccoli et al.: “Alternative Measurements Techniques for LEO-LEO Radio Occultation (AlMeTLEO)” ESA-ESTEC contract No. 17831/03/NL/FF Final report, July 2004
2. L. Facheris, E. Martini, F. Cuccoli, F. Argenti, ”Differential spectral attenuation measurements at microwaves in a LEO-LEO satellites radio occultation geometry: a novel approach for limiting scintillation effects in tropospheric water vapor measurements” Proc. SPIE Conf. "Microwave Remote Sensing of the Atmosphere and Environment IV", Honolulu, Hawaii, USA, 9-11 Nov. 2004, Vol. 5654, pp. 232-243.
3. F. Cuccoli, L. Facheris, S.Tanelli and D.Giuli, "Microwave attenuation measurements in satellite-ground links: the potential of spectral analysis for water vapor profiles retrieval" IEEE Transactions on Geoscience and Remote Sensing, Vol. 39, No 3, March 2001, pp. 645-654
4. F. Cuccoli, L. Facheris, "Estimate of the tropospherical water vapor through microwave attenuation measurements in atmosphere" IEEE Transactions on Geoscience and Remote Sensing, Vol. 40, 4, April 2002, pp. 735 – 741.
5. H.J. Liebe, G.A. Hufford, M.G. Cotton “Propagation Modeling of Moist Air And Suspended Water/Ice Particles at Frequencies below 1000 GHz”, in AGARD 52nd Specialists Meeting of the Electromagnetic Wave Propagation Panel on “Atmospheric Propagation Effects through Natural and Man-Made Obscurants for Visible to MM-Wave Radiation”, Palma de Mallorca, Spain, May 1993
6. http://raob.fsl.noaa.gov/: web site of FSL/NCDC (Forecast Systems Laboratory/National Climatic Data Center) radiosonde data archive